HHS Public Access

Author manuscript

Cell Rep. Author manuscript; available in PMC 2026 April 01.

Published in final edited form as:

Cell Rep. 2026 February 24; 45(2): 116892. doi:10.1016/j.celrep.2025.116892.

Stress testing reveals selective vulnerabilities in protein homeostasis

Berent Aldikacti[1,2], **Hidayet Putun**[1,2], **Vishal Sarsani**[4], **Rilee Zeinert**[5], **Patrick Flaherty**[3], **Peter Chien**[1,2,6,7,*]

[1]Molecular and Cellular Biology Program, University of Massachusetts Amherst, Amherst, MA, USA

[2]Biochemistry and Molecular Biology Department, University of Massachusetts Amherst, Amherst, MA, USA

[3]Department of Mathematics and Statistics, University of Massachusetts Amherst, Amherst, MA, USA

[4]Broad Institute, Harvard/MIT, Cambridge, MA, USA

[5]Division of Molecular and Cellular Biology, Eunice Kennedy Shriver National Institute of Child Health and Human Development, National Institutes of Health, Bethesda, MD, USA

[6]Senior author

[7]Lead contact

SUMMARY

Protein quality control (PQC) systems are essential for cellular resilience to proteotoxic stress. Despite intensive study, functional redundancies in the system obscure the contributions of important individual genes. Here, we leverage transposon sequencing (Tn-seq) across bacterial strains lacking key chaperones and proteases to reveal hidden determinants of stress response in protein homeostasis. By profiling fitness under multiple proteotoxic stresses, we uncover stress-specific vulnerabilities and reveal how major players of PQC mask correlations between transcriptomic responses and gene fitness. We identify a heat-specific synthetic lethality between the ClpB disaggregase and DNA polymerase 1 mediated by prolific aggregation of the RecA recombinase and persistent induction of the heat shock regulon, supporting a conclusion that vulnerabilities in PQC are genetic- and environmental-context specific. Overall, our work presents a framework to reveal critical addressable fragilities in stress responses using gene fitness scores adaptable to a variety of systems.

*Correspondence: pchien@umass.edu.

AUTHOR CONTRIBUTIONS

Conceptualization, B.A. and P.C.; methodology, B.A. and P.C.; investigation, B.A., H.P., V.S., R.Z., P.F., and P.C.; writing – original draft, B.A. and P.C.; writing – review & editing, B.A., H.P., V.S., R.Z., P.F., and P.C.; funding acquisition, P.F. and P.C.; resources, P.C.; supervision, P.F. and P.C.

DECLARATION OF INTERESTS

The authors declare no competing interests.

In brief

Aldikacti et al. use fitness landscapes to explore proteostasis under stress and uncover genetic factors that become essential when key protein quality control systems are compromised. They highlight how aggregation of specific proteins drives lethal vulnerabilities in particular genetic or environmental backgrounds, advancing our understanding of stress resilience mechanisms.

Graphical Abstract

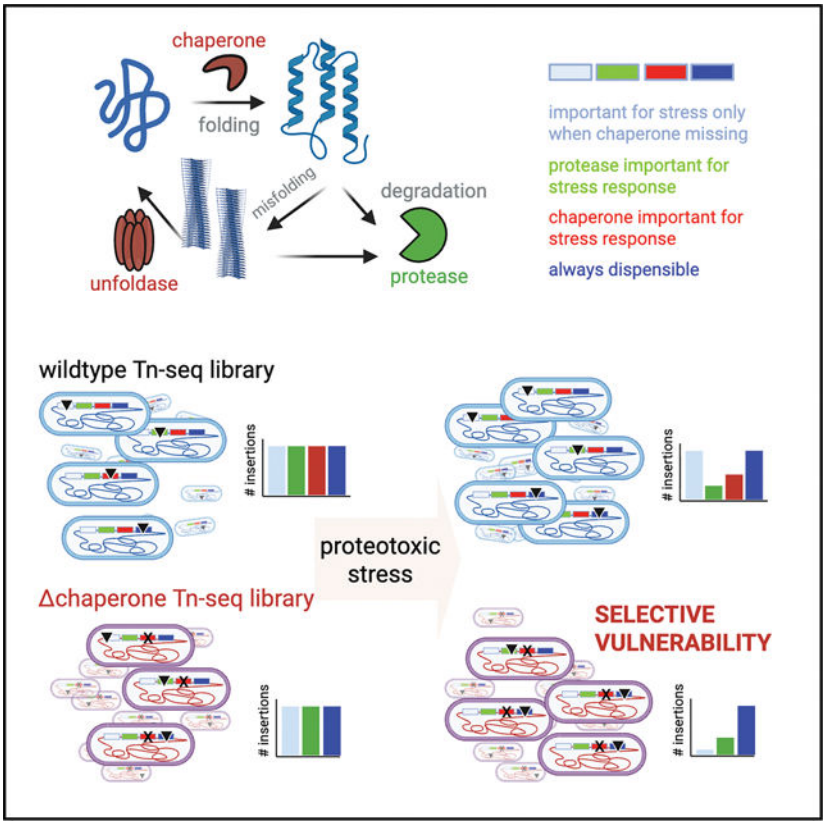

INTRODUCTION

Protein quality control (PQC) is critical for cell homeostasis across all life. Networks of molecular chaperones and proteases balance protein synthesis, folding, maturation, and degradation to maintain a healthy proteome. Disruption of human PQC results in several pathologies, such as neurodegenerative diseases,[1,2] cancer,[3] and aging.[4,5] In bacteria, loss of PQC components affects normal cell growth,[6–8] stress responses,[8–11] and host interactions.[9]

Mutagenesis screens have been widely used to identify the phenotypic consequences of genetic perturbations. Methods such as transposon insertion sequencing (Tn-seq) or CRISPRi have been used to identify the phenotypic profiles of single-gene knockouts or knockdowns on a genome-wide scale. These approaches have led to the discovery of new virulence factors,[12,13] membrane integrity elements, motility genes,[14] and whole-genome essentiality maps of several bacteria.[15,16] However, due to the crosstalk between pathways

and redundancies in biological systems, most genes do not show phenotypic consequences in single-gene knockouts.[17–22]

Simply put, while a gene may be necessary for a stress response, deletion of only this gene may not result in an observable phenotype because redundancy in the networks will compensate for this loss. Consequently, numerous genes remain either “hypothetical” or annotated based on structural similarity, even in organisms that have been extensively studied and have well-annotated genomes.[23] To reveal the functions of genes whose function is obscured by redundancy, there have been recent developments, such as dual CRISPRi-seq[24] and dual Tn-seq,[25] to interrogate gene-gene interactions on a genome-wide scale. Additionally, many gene phenotypes can only be revealed during stress. For example, the disaggregase ClpB does not show any phenotype under normal growth conditions; however, it is essential under acute heat stress.[26–28]

We reasoned that combining known PQC stresses under conditions where known response factors are compromised would reveal insight into protein homeostasis akin to failure mode analysis in engineering, which reveals the robustness of a system once specific components have been weakened. Specifically, we interrogate genome-wide fitness of Tn-seq libraries generated in strains missing major chaperones and proteases under known proteotoxic stress conditions (Figure 1A). Through this approach, we identify genes that are important to the global stress response, robust against perturbations in quality control pathways, and sensitive to perturbations in specific PQC pathways. We identify redundancies in PQC that normally mask the correlation of transcriptional and phenotypic consequences of stress response genes. Finally, we identify an unexpected synergy between heat stress-induced protein aggregation and the DNA damage response, which exposes how cells become vulnerable during heat stress due to specific environmental or genetic pressures rather than a generic defect in fitness. Taken together, our work serves as an exemplar of combining systems-wide fitness surveys with a deliberate focus on specific stresses to reveal novel insights.

RESULTS

Phenotypic fitness profiling for studying PQC network

PQC stress responses rely on the presence of chaperones and proteases that mitigate proteotoxicity. Major players of this stress response are known, such as Hsp70 chaperones and disaggregases, that are the primary responders to the misfolded protein burden.[29,30] How additional players shape this response is less known, in part because of the dominance of these major players. We reasoned that a multiplexed reverse genetic screen approach such as Tn-seq conducted in cells lacking major PQC responders and subjected to proteotoxic stresses would identify fitness determinants that may be hidden or redundant. While PQC systems range in components across systems, the core of the PQC system is preserved in bacteria.[31,32] Given this conservation, we used *Caulobacter crescentus* (*Caulobacter*) in our current approach.

We previously generated dense transposon mutagenesis libraries from five strains, including loss of proteases (Lon and ClpA) and loss of normal chaperone activity (ClpA, ClpB, and DnaK).[33] We subjected these mutagenesis libraries to three proteotoxic stressors at three

different stress levels: heat stress, which causes misfolding, degradation, and DNA damage; oxidative stress, which oxidizes proteins and causes misfolding and DNA damage[34,35]; and L-canavanine, an L-arginine analog that leads to protein misfolding upon incorporation into polypeptides. A Bayesian analysis of this dataset exposed the overall structure of the data, showcasing synergistic connections between strains and stress conditions, but lacked specific molecular insights due to the nature of this initial global analysis.[33]

To explore this dataset in a more candidate-focused manner, we first identified genes that affected fitness for a given stress in all strains (Figure 1B). For example, ClpB is the Hsp104-family ATP-dependent disaggregase needed to resolve heat-induced protein aggregates.[28,32] As expected, *clpB* is identified as a fitness determinant in all strains, specifically under heat stress, which we validated by constructing clpB deletions in all strains and performed growth assays of these double mutants (Figures 1C and S1A). Similarly, KatG is the only known peroxide-detoxifying catalase in *Caulobacter. W*e find that *katG* is identified as a fitness determinant in all strains, specifically under oxidative stress (Figures 1D and S1B).

For canavanine stress, we find *CCNA_02154* (renamed CanA) as a fitness determinant in all strains, which we validate using double mutant strain growth curves (Figures 1E and S1C). We considered if increased sensitivity to canavanine was due to excess incorporation of this specific unnatural amino acid or toxic consequences from prolific levels of aberrantly folded polypeptides. In agreement with the first possibility, loss of *canA* does not increase sensitivity to azetidine-2-carboxylic acid (AZC), a proline analog that is also misincorporated and leads to proteome-wide misfolding (Figure 1F). Given that CanA is annotated as a putative acetyltransferase and its selective effects on canavanine, we hypothesized that acetylation of canavanine may prevent its incorporation into polypeptides. Consistent with this model, CCNA_02153, the gene adjacent to *canA*, is annotated as a deacetylase, and based on Tn-seq, loss of this gene protects against canavanine toxicity (Figure S2).

The genes *clpB, katG,* and *canA* are all examples of determinants that are universally important for one stress response (heat, oxidative, and canavanine, respectively) but do not show reproducible fitness differences under the other tested proteotoxic stresses (Figure 1B). We found additional genes that show this same degree of universal stress specificity (Table S1). We also identify examples of genes being important for more than one response (Table S1). For example, *dps* (*CCNA_02966*) encodes the ferritin-like DNA-binding protein and emerges as a fitness determinant for both oxidative and heat stress in our studies, consistent with work from other bacteria.[36,37] We validated the dual stress intolerances of *dps* in *Caulobacter* by constructing double mutants and find sensitivity to both peroxide and heat in all strains (Figure S3). Finally, we tested if any genes were fitness determinants in all stresses and all strains. While no genes passed this filter, we identified 18 fitness determinants for all proteotoxic stresses tested in several strain combinations (Table S1). This indicates that no global fitness determinants are important for all tested PQC stresses that function entirely independently of the chaperones and proteases examined in this study.

Loss of Lon highlights synergies between DNA damage and oxidative stress responses

Given the depth of the dataset, we next explored subsets of genes known to be regulated by proteotoxic stresses, focusing on the known transcriptional response to oxidative stress.[38] In wild-type cells, we found that most genes that are transcriptionally upregulated during oxidative stress do not contribute to tolerance of that stress (Figure 2A). A similar, originally surprising, lack of correlation between transcriptomic and fitness profiles of genes has been reported in other systems,[18,39] leading to a natural conclusion that genes needed for stress tolerance should already be expressed at levels needed to withstand that stress prior to the insult. Interestingly, we find that a subset of these upregulated genes, which includes DNA damage repair proteins, are revealed as important for oxidative stress tolerance in the absence of the Lon protease (Figure 2B). In addition to damaging proteins, oxidative stress also causes genotoxic damage, which must be rescued by DNA repair proteins. Our interpretation of the results in Figure 2B is that in the wild-type cells, there is sufficient capacity to withstand this amount of genotoxic damage even in the absence of individual repair proteins, reflecting the lack of fitness defects seen in our Tn-seq results. However, when Lon is missing, cells are already deficient in DNA repair responses such that loss of individual genes becomes more striking. This result reflects the strength of our approach using multiple strains, as this link was only evident in cells lacking the Lon protease (Figure 2C).

We validate the link between Lon, oxidative stress, and the need for DNA repair proteins by performing competition growth assays. RecA is the recombinase critical for many aspects of DNA damage and is one member of the Lon-specific oxidative stress-sensitive gene sets (Figures 2B and 2C). We generated cells lacking *recA* or *lon* or both, then fluorescently tagged strains with mVenus to visualize populations of different strains upon coculture growth. We find that loss of *recA* does not affect competitive growth compared to wild-type cells following oxidative stress, but Δ*lon* strains lacking *recA* do worse than Δ*lon* cells alone under stress conditions (Figure 2D). In addition, monitoring the growth of monocultures of each strain, *ΔlonΔrecA* show a synergistic sensitivity to oxidative damage (Figure S4). We conclude that upregulation of DNA damage response genes is an important aspect of the oxidative stress response, but a Lon-dependent pathway normally masks its phenotypic importance.

Similar analysis with other transcriptional responses, such as the heat stress regulon controlled by RpoH,[42,43] also exposes the importance of specific genes in conditional backgrounds, with greater numbers of genes emerging as important during heat stress in specific strains (Figures 2E and S5). For example, the oxidative stress gene *CCNA_03496* (*yaaA*)[44,45] emerges as important for heat stress tolerance, specifically in a Δ*clpB* background, but not other strains, suggesting a link between heat and oxidative stress when ClpB is lost that differs from other strains (Figure S6A). Our prior work supports that Δ*clpB* strains are altered in oxidative stress response during low heat stress compared to wild-type strains,[33] consistent with the selective gene fitness in this current analysis. We also see connections with multiple PQC-deficient backgrounds; for example, *CCNA_03811* (*oxyR*)[38] appears important for heat stress in both Δ*clpB* and Δ*lon* (Figure S6B). Similar analyses will

provide a rich starting ground for experiments to test new hypotheses regarding the PQC system in bacteria.

Loss of DNA polymerase 1 and ClpB are synthetically lethal during heat stress

During our examination of strain-specific stress responses, we noticed that loss of DNA polymerase 1 (*polA; CCNA_03577*) resulted in both oxidative- and heat-stress sensitivity in our datasets. Interestingly, in a Δ*clpB* background, there was a 24-fold loss in *polA* insertions during heat stress compared to a 3-fold loss during oxidative stress (Figure 3A), i.e., heat tolerance was 8-fold worse than oxidative stress tolerance. In comparison, a similar examination of Tn counts for Δ*clpA* shows a 2-fold fitness defect in heat tolerance compared to oxidative stress, and a similarly reduced difference was seen in the other strains. Therefore, we decided to follow up on this observation to explore if there was a specific synthetic effect between *clpB* and *polA* during heat stress. PolA is the first discovered DNA polymerase[46] and plays a crucial role in DNA replication and repair, mainly due to its function in the formation of Okazaki fragments.[47] In *Escherichia coli*, upregulation of *polA* is part of the DNA damage (or SOS) response, and deletion of *polA* results in sensitivity to DNA damage, heat, and oxidative stress.[48,49] We identified similar defects for a Δ*polA* strain of *Caulobacter* (Figures 3B–3D). Consistent with the Tn-seq results, loss of *polA* in a Δ*clpB* background resulted in a synergistic sensitivity to heat stress (Figures 3C and S7).

We next addressed whether this synergistic effect was limited to heat stress. PolA is known to be important for DNA damage and oxidative damage, and while we found this to be true in Caulobacter, we found no synergy of loss of PolA with loss of ClpB in these stresses (Figures 3B and 3D). Similarly, other known defects of Δ*clpB*, such as sensitivity to ethanol,[28] were not enhanced in the absence of PolA (Figure 3E). We conclude that the synergistic fitness defect we find between ClpB and PolA is exclusive to heat stress and sought to understand if this was due to a systems-level or molecular-level defect.

Persistent upregulation of the heat-stress regulon is toxic in the absence of PolA

To explore a systems-level basis of this synergistic fitness defect, we used RNA sequencing to compare the transcriptomic profile of wild-type and Δ*clpB* strains during moderate heat-stress conditions. We found 72 genes up-regulated, and 45 down-regulated in Δ*clpB* under moderate heat stress (FDR <0.05; Table S3). We reasoned that synthetic fitness effects could arise from lower expression of factors needed in a Δ*polA* background or intoxication due to overexpressed factors. Of the downregulated genes, we focused on the *imuABC* operon, which encodes a mutagenic polymerase, because this operon, along with other SOS response genes, is also upregulated in the Δ*polA* strain based on RNA-seq (Figure S8; Table S3), suggesting its loss may explain the synthetic sickness of the double mutant. However, deletion of *imuC* (also known as *dnaE2*[50,51]) in a Δ*polA* background showed no synthetic phenotype even with heat stress (Figure S9). We, therefore, turned our attention to the genes upregulated during heat stress in Δ*clpB*.

In bacteria, transcriptional changes due to heat stress are primarily driven by the sigma factor RpoH.[52–54] Prior studies in *Caulobacter* suggest that ClpB is needed for reactivation

of the housekeeping sigma factor RpoD following heat stress,[28] which would result in the eviction of the unstable heat-shock sigma factor RpoH from the RNAP complex during the recovery phase. Consistent with this interpretation, we found that nearly all of the up-regulated genes in Δ*clpB* strains can be explained by the RpoH-dependent regulon[42] (Figure 4A). We considered whether persistent expression of the heat-stress regulon may underlie some of the synthetic lethality we see between ClpB and PolA during heat stress. Upregulation of RpoH is well tolerated in wild-type cells, but expression of a stabilized active variant of RpoH (RpoH-V56A) results in lethality. Interestingly, in cells lacking PolA, even the upregulation of wild-type RpoH causes lethality (Figures 4B and S10), suggesting that Δ*polA* strains are particularly sensitive to excess RpoH activity.

Because the SOS regulon is persistently upregulated in Δ*polA* and the heat-shock regulon is persistently upregulated in Δ*clpB*, we wondered whether transcriptional conflicts between these regulons might contribute to the PolA-ClpB phenotype. To test this, we primed Δ*clpB* cells with UV stress to induce the SOS response and then exposed them to heat stress. In contrast to a model where elevated SOS responses conflict with the heat-stress regulon, our results indicated that activation of the SOS response provided protection against heat stress (Figure S11A). This suggests that persistent upregulation of the SOS response in Δ*polA* cells does not contribute to the synergy between PolA and ClpB that results in reduced heat-stress tolerance.

Loss of ClpB results in sensitivity to immediate DNA damage upon heat stress

Given the known genotoxic sensitivity of Δ*polA* and the synergy between PolA/ClpB, we explored links between DNA damage and ClpB-mediated protection from heat stress. Interestingly, cells were more sensitive to the DNA-damaging agent mitomycin C (MMC) immediately after heat stress but lost this sensitivity following an 8-h recovery after heat stress. This effect was more pronounced in the Δ*clpB* strain (Figure 4C), suggesting that the failure to recover after heat stress and increased sensitivity to immediate DNA damage might be linked. Because RpoH-dependent expression is persistent in Δ*clpB* (Figure 4A) during moderate heat stress, we tested whether this persistence could be the root cause of the DNA damage sensitivity. We found that cells expressing RpoH variants were no more sensitive to DNA damage than cells with control plasmids (Figure S11B). Therefore, while elevated RpoH-dependent expression explains some features of the Δ*clpB* defects, it is insufficient to explain this immediate DNA damage sensitivity. Because ClpB is primarily known as a disaggregase, we explored whether aggregation of specific proteins could underlie this phenomenon.

Heat-induced aggregation of specific proteins contributes to the PolA-ClpB phenotype

Prior work identified several proteins aggregated during heat stress in *Caulobacter*, including GyrA and RecA,[55] both important for DNA replication and repair. In *E. coli,* genetic studies suggest that *polA* and *recA* are synthetically lethal.[56,57] Building on this, we hypothesized that the sequestration of RecA in insoluble protein aggregates might contribute to the synergistic effect between PolA and ClpB, as cells lacking ClpB fail to resolve their aggregates. This hypothesis would require that *ΔpolA* and Δ*recA* show synthetic fitness effects. Initial attempts to generate double mutants failed, which is consistent with a need for

both genes. We were able to construct Δ*polA*Δ*recA* strains in the presence of an integrated copy of *recA* at a separate locus under inducible control. Removal of the inducer resulted in cell death, which is consistent with a synthetic lethal effect due to the loss of both RecA and PolA (Figure 5A). Armed with this knowledge, we next explored if this synthetic lethality underlies the synergistic defect of Δ*polA*Δ*clpB* during heat stress.

We measured insoluble RecA levels during heat stress using centrifugation of extracts before heat stress and during recovery and then detected RecA with specific antibodies. In Δ*polA* strains, soluble RecA levels were elevated under basal conditions, consistent with an increased need for this protein in the absence of DNA polymerase I and the increased transcription of the SOS response (Figure S8). As predicted, acute heat stress caused aggregation of many proteins, including RecA (Figures 5B and 5C). In cells with wild-type ClpB activity, these aggregates were resolubilized over time, whereas in the absence of ClpB, aggregates were persistent. Western blots confirmed that RecA was also retained in aggregates in the absence of ClpB (Figure 5C). We conclude that prolonged loss of soluble RecA in the Δ*polA*Δ*clpB* strain following heat stress contributes to the heat stress specific synthetic lethality in this double mutant.

Given that Δ*clpB* strains show persistent aggregation of many proteins but are more fit than Δ*polA*Δ*clpB* strains following heat stress, we propose that heat stress-induced aggregation alone is not itself toxic. Instead, the aggregation of particular proteins (such as RecA) is toxic only under certain genetic backgrounds (such as Δ*polA*) or additional stresses (such as MMC) that make the strain under those conditions vulnerable to that specific loss. Given this rationale, other heat-stress-driven synthetic lethalities only in Δ*clpB* might reflect these additional vulnerabilities. For example, the importance of oxidative stress factors YaaA and OxyR for tolerating high heat stress in Δ*clpB* described earlier (Figures S6A and S6B) may be due to the aggregation of redundant proteins important for the oxidative stress response that fail to be rescued in the absence of ClpB.

DISCUSSION

This study demonstrates how targeted transposon sequencing can reveal critical insights into PQC mechanisms in proteotoxic stress conditions. By perturbing PQC pathways and subjecting cells to various stressors, we identified new genetic determinants of stress resilience and uncovered condition-specific vulnerabilities. Specifically, we identified new genes important for stress responses, demonstrated how redundancies in the stress response mask the importance of important genes, and demonstrated that loss of viability due to aggregation results from condition-specific vulnerability rather than general aggregation (Figure 6).

Our approach successfully identified genes contributing to stress resilience beyond the well-characterized PQC machinery. Due to functional redundancy within stress-response networks, traditional single-gene knockout studies often fail to reveal phenotypic consequences. However, by examining mutant libraries in backgrounds lacking key PQC components, we unearthed previously unrecognized fitness determinants under specific stress conditions. For instance, we identified CanA as a critical factor selective for

canavanine stress, likely through acetylation of the unnatural amino acid and a neighboring predicted deacetylase that limits this protective activity. We also revealed the importance of Dps in both heat and oxidative stress in all strains regardless of PQC status, highlighting the ability of this method to uncover stress-specific genes that are otherwise masked in wild-type conditions.

We observed that many genes upregulated in response to stress do not necessarily contribute to stress tolerance under normal conditions. Instead, their importance becomes evident when key stress-response genes are absent. This was particularly apparent in the case of oxidative stress, where genes involved in DNA repair became critical only in the absence of the Lon protease. This suggests that transcriptional upregulation does not always equate to functional necessity but may serve as a compensatory mechanism only required under specific genetic perturbations.

Our findings suggest that cellular sensitivity to stress is likely due to the loss of specific crucial proteins, the consequences of which are particular to the specific state of the cell, rather than a general consequence of protein aggregation. The cell state depends on both genetic background and the type of stress applied. For example, heat-induced protein aggregation sequesters a number of specific proteins, loss of which could be toxic under specific conditions. Specifically, we found that the heat-induced persistent aggregation of RecA (or possibly, increased filamentation of RecA) in the absence of the ClpB protein leads to a synthetic lethal outcome in a polA-deficient background or when cells immediately encounter genotoxic conditions during heat stress. Extending this result suggests that the detrimental effects of stress may primarily arise from the loss of specific proteins whose absence becomes particularly deleterious under defined genetic or environmental contexts, rather than a general overall loss in fitness. For example, CCNA_03872, a tRNA synthase, appears especially critical during heat stress in Δ*clpB*, and *CCNA_03201*, an adenylosuccinate synthetase shows synergies during heat stress with Δ*clpB* and Δ*clpA* (https://chienbrowser.biochem.umass.edu/chienlab/chienlab_prod2021/). In these cases, we predict that key partner proteins needed in either translation or purine biosynthesis may also be persistently aggregated during heat stress.

In summary, our study underscores the power of using systematic mutagenesis in perturbed backgrounds to elucidate hidden stress response mechanisms. By identifying novel stress determinants, decoupling gene expression from functional necessity, and linking stress sensitivity to the selective loss of key proteins, we provide a refined understanding of bacterial stress responses that can inform future studies in both fundamental and applied microbiology. For example, similar approaches with antibiotic stresses and known resistance genes will allow us to identify additional pathways to target, which is especially important given the alarming rise of antibiotic resistance in many human pathogens.

Limitations of the study

Here, we show a targeted transposon mutagenesis study in perturbed PQC backgrounds to uncover hidden fitness determinants and novel interactions. However, Tn-seq has intrinsic limitations, such as small genes, essential genes with dispensable domains, and nucleoid-associated proteins.[58–61] These issues can result in false-positive or -negative results.

Additionally, it is only possible to study interactions involving genes that can be knocked out.

Furthermore, in our study design, we focus on the effect of transposon insertion alongside stress effects. In non-wild-type strains, there is also the addition of the background strain. The combination of multiple insults makes it difficult to distinguish between direct and indirect effects.

Another limitation is potential species-specific effects. In this study, we have only examined the phenotype of our model organism, *Caulobacter crescentus*. The heat- and oxidative-stress sensitivity of PolA has been shown in *E. coli*,[49] and the heat-stress sensitivity of Δ*clpB* is conserved,[26,27,62,63] but it is possible that the PolA-ClpB synergistic phenotype is Caulobacter-specific.

Finally, we provided mechanistic evidence for PolA's heat-stress phenotype and its synergistic relationship with ClpB, including RpoH overexpression and RecA aggregation. However, further studies, including deletion studies, are still needed to explain the deeper mechanistic reasons why RpoH overexpression causes a fitness defect in the Δ*polA* background and the exact function of PolA that leads to these defects.

RESOURCE AVAILABILITY

Lead contact

Further information and requests for resources and reagents should be directed to and will be fulfilled by the lead contact, Peter Chien (pchien@umass.edu).

Materials availability

Materials generated in this study are listed in the key resources table and available from the lead contact.

Data and code availability

• RNAseq data have been deposited at GEO at GSE312471 accession number and are publicly available as of the date of publication.

• RNAseq alignment and annotation pipeline can be found in our GitHub repository (https://github.com/baldikacti/chienlab-rnaseq) (Zenodo: https://doi.org/10.5281/zenodo.17809427).

• Tnseq alignment and annotation pipeline can be found in our GitHub repository (https://github.com/baldikacti/chienlab-tnseq) (Zenodo: https://doi.org/10.5281/zenodo.17852222).

• A web-based application to explore Tnseq data results is hosted from the UMass BMB Department's server (https://chienbrowser.biochem.umass.edu/chienlab/chienlab_prod2021/).

• Any additional information required to reanalyze the data reported in this paper is available from the lead contact upon request.

STAR★METHODS

EXPERIMENTAL MODEL AND STUDY PARTICIPANT DETAILS

Caulobacter crescentus strains

Bacterial strains and plasmids used in this study are listed in the key resources table. Every mutant *Caulobacter* strain generated from the original NA1000 (WT) strain and grown in PYE medium (2 g/L peptone, 1 g/L yeast extract, 1 mM MgSO4, and 0.5 mM CaCl2) with aeration at 30°C unless otherwise noted. Antibiotic selections performed at the following concentrations (agar-liquid); kanamycin (25–5 μg/mL), gentamycin (5–0.5 μg/mL), tetracycline (2–1 μg/mL), spectromycin (100–25 μg/mL), streptomycin (5–5 μg/mL), chloremphenicol (1–1 μg/mL).

For plasmid generation, TOP10 *Escherichia coli* competent cells were grown in LB broth (10g/L NaCl, 10g/L tryptone, 5g/L yeast extract) and supplemented with kanamycin (50 μg/mL), gentamycin (40 μg/mL), or spectromycin (50 μg/mL), streptomycin (100 μg/mL) when necessary.

Cloning and strain construction

Single gene knockouts performed by two-step recombination method with sucrose counter selection using pNTPS138 plasmid.[78] To make *ΔpolA* and *ΔkatG* strains, pNTPS138 plasmid digested using HindIII and EcoRI restriction enzymes and subsequently gel purified. Around 1000 bp upstream and downstream (5′UTR & 3′UTR) regions of the *polA* or *katG* gene and the GENT resistance cassette were PCR amplified. The pNTPS138 plasmid and amplified fragments combined using Gibson Assembly and transformed into TOP10 E.Coli competent cells. The resulting plasmid transformed into electrocompotent NA1000 (*WT*) strain and primary selection perform in PYE agar supplemented with kanamycin. Colonies from the primary selection grown overnight in PYE and plated on PYE agar supplemented with 3% w/v sucrose and gentamicin for secondary selection. Finally, colonies from the secondary selection plated on both PYE agar supplemented with kanamycin or gentamicin, and only colonies which grew on gentamicin but not kanamycin plates were harvested as potential Δ*polA* or *ΔkatG* strains.

All the double knock-out strains were generated using PhiCr30 phage transduction as described before with slight modifications.[79] Phage lysates from the donor strains obtained by mixing the 0.5mL of the donor strain at three different concentration of phage at; 50, 5, and 0.5μL. After 15 min of incubation at room temperature, cell:phage mixture added to 4mL of molten soft PYE agar (0.3%) and poured on a plate with solidified PYE agar (1.5%). After overnight incubation, soft agar scraped and resuspended with 5 mL of PYE, rigorously vortexed for 2 min, 0.1mL of chloroform added, and centrifuged at 8000g for 30 min to get rid of remaining donor cells. The supernatant stored at 4°C as the phage lysate for further use. To move the mutation from donor strain to receiver strain, 1 mL of the phage lysate from the donor strain UV treated at 1.2 joules and mixed with the receiver strain at 1:4 ratio. (50:200μL) The mixture incubated at room temperature for 1 h and spread on PYE agar plates supplemented with gentamicin, tetracycline, or chloramphenicol.

METHOD DETAILS

Transposon mutagenesis library generation

Transposon mutagenesis libraries used in this study were generated as previously described.[33,80] Briefly, *E.coli* cells containing randomly barcoded EZTn5 plasmids (APA752, gift from Deutschbauer lab) are conjugated with *WT, Δlon, ΔclpA, ΔclpB, and dnaK-NI* (Xylose-inducible *dnaK*) *Caulobacter crescentus* cells separately. *E.coli* donors are kanamycin-resistant and diaminopimelate (DAP) auxotrophs and require it in the media to grow. For conjugation, E.*coli* donor cells Caulobacter strains were mixed at a 1:10 ratio overnight on a PYE agar plate supplemented with DAP (300 μM). The next day, the conjugate was scraped, resuspended, and spread over 14 large (150 × 15 mm) PYE agar plates supplemented with kanamycin (25μg/ml) and without DAP per strain. In this culture, the donor cells will not survive due to no DAP, and acceptor Caulobacter cells will be selected for the Tn5 plasmid due to kanamycin selection. Colonies were scraped, pooled, and frozen in PYE +10% glycerol in 1 mL aliquots. For stress condition experiments, 1 aliquot per replicate per strain was thawed in 3.5 mL of PYE or PYE+%0.2 xylose and recovered overnight in a 30 ℃ shaker. For all *dnaK-NI* experiments, cells were recovered at saturating xylose concentrations (PYE+%0.2 xylose), and the stress experiments were done at minimal xylose concentrations. (PYE+%0.002) All conditions were performed in quadruplicates, and optical density (OD) measurements were taken at 600nm. Experiments were done in multiple batches.

Transposon mutagenesis experiments

Control environment: Libraries were back diluted to OD 0.008 into 7 mL of PYE or PYE+0.002% xylose and grown overnight until they reached saturation at OD ~1.6.

Heat stress: Libraries diluted to OD of 1 and heat-stressed at low, medium, or high (37, 42, 43.8°C, respectively) for 45 min in a Biorad Thermocycler. After 45 min, cells diluted back to final OD of 0.008 in 7 mL media for 24-h growth.

Oxidative stress: Libraries were directly diluted back to OD of 0.008 in 7 mL media that contains low, medium, or high (0.025mM, 0.05mM, 0.1mM) level hydrogen peroxide. Cells were grown for 24 h in these chronic stress conditions.

Canavanine stress: Libraries were directly diluted back to OD of 0.008 in 7 mL media that contains low, medium, or high (25ng/ml, 50ng/ml, 100ng/ml) level hydrogen peroxide. Cells were grown for 24 h in these chronic stress conditions.

Transposon sequencing PCR library preparation and sequencing

The sequencing libraries for Next-generation sequencing were prepared using a customized three-step PCR protocol (PCR1–2-3). Genomic DNA input was normalized to a concentration of 100 ng/μL. The initial transposon junction amplification (PCR1) was performed using an arbitrary PCR amplification method. This step utilized a forward primer designed (PCR1_F_RBTn5) to align with one end of the transposon and three reverse arbitrary primers (PCR1_R_arb1–2-3). The PCR1 process employed a 2-step cycling

protocol with annealing temperatures set at 42°C and 58°C and the number of cycles at 6 and 15, respectively. Subsequently, the second PCR step (PCR2) involved the addition of 16S adapters for Illumina indexing, along with unique molecular identifiers (UMI), and amplification of the library for 36 cycles. Post-PCR2 cleanup was performed using Aline PCRClean DX magnetic beads. The final PCR step (PCR3) incorporated NexteraXT dual indexes in accordance with the manufacturer's protocol. Post-indexed library (PCR3) cleanup was performed using Aline PCRClean DX magnetic beads.

Transposon sequencing data analysis

DNA libraries were sequenced in 5 batches with Illumina NextSeq 500 instrument using the NextSeq High output v2.5 single-end 75bp kit. Resulting *fastq* files pruned using a static region from the transposon (TGTATAAGAG) with *seqkit*,[70] PCR duplicates removed with *JE*,[69] reads aligned to NA1000 (NC011916.1) reference genome with *bwa-mem*,[66] and genome positions assigned to the 5′ positions of transposon insertions with *bedtools genomecov*.[68] Subsequently, *bedtools map* used to count either the total or unique transposon insertion counts with either *bedtools map -o sum* or *bedtools map -o count*. For mapping, we used a reference file in which the genes were clipped by 10% from the N and C terminal regions to eliminate spurious transposon insertions in the terminal regions. A snakemake[74] pipeline of the Tnseq preprocessing/alignment/mapping is available at our GitHub repository. (https://github.com/baldikacti/chienlab-tnseq).

We have applied ComBat-Seq[77] batchcorrection to the raw counts to minimize the batch effects introduced by the separate sequencing runs.

RNA sequencing experiments

RNAseq experiments were performed in chronic heat-stress conditions in 96-well plates in a microplatereader. *WT*, Δ*clpB*, and Δ*polA* strains grown overnight in PYE and back-diluted to 0.1 OD in the morning. Back-diluted cells subsequently plated in a 96-well plate in triplicates (200µL/well) where each replicate was plated to 9 different wells each to get enough final volume. Cells were grown in the plate reader until the mid-log phase at 30°C or 39°C. Finally, the wells with the replicates combined separately, pelleted, and snap frozen.

RNA sequencing and analysis

Cell pellets from the RNAseq experiments sent to SeqCenter, LLC for RNA isolation. library preparation, and sequencing. Library preparation was performed using Illumina's Stranded TotalRNA Prep Ligation with Ribo-Zero Plus kit with custom primers for depleting Caulobacter rRNA. Sequencing was done on a NovaSeq X Plus, producing paired end 150bp reads. Demultiplexing, quality control, and adapter trimming was performed with bcl-convert (Illumina).

RNAseq read alignment and mapping was done using a custom pipeline. Briefly, read quality control and filtering performed using *fastq*,[72] reads aligned to reference genome with *bwa-mem*,[66] read quantification performed with *rsubread*,[73] bigwig files generated for manual visualization in genome browsers using *deeptools*,[71] and finally, principal

component analysis (PCA) and differential expression analysis performed using *DESeq2*.[81] The custom pipeline is available at https://github.com/baldikacti/chienlab-rnaseq.

For RNAseq data of Silva et al.,[38] the raw sequence files (fastq) were downloaded from NCBI's Sequence Read Archive (SRA:SRP148432). The alignment, mapping, and differential expression analysis were performed using the chienlab-rnaseq pipeline as described above.

Growth curve experiments

Growth curve experiments were carried out using a 96-well in a BioTek Epoch microplate reader (Gen6 software). Overnight or log phase cultures are initially diluted to OD 1 for acute stresses and subsequently diluted to OD 0.008 in 96-well plates (in 200 μL) with inducers, antibiotics, and stresses, as needed. The plates were cultured at 30°C and continuous linear shake (330 ppm) for 24 h unless otherwise noted. Measurements were taken at OD600 every 20 min. All experiments were performed with three biological replicates.

Spot titration experiments

Overnight or log phase cultures were initially diluted to OD 1 for acute stresses and subsequently diluted to OD 0.1 and made 8 10x titrations in a 96-well plate. 3 μL aliquots from serial dilutions were spotted on PYE agar plates using a multi-channel pipette. PYE agar plates contained inducers, antibiotics, and stresses, as needed. Spot plates were cultured in a 30°C incubator for 2–3 days and imaged using a Syngene G:Box. All experiments were performed with three biological replicates unless otherwise noted.

Competition experiments

For competition experiments, the overnight cultures of *WT* and Δ*recA* strains mixed with *WT::venus* strain and Δ*lon* and Δ*lon*Δ*recA* strains mixed with Δ*lon::venus* strain at a 1:1 ratio. The mixtures were inoculated into 5 mL of PYE media at a final OD of 0.0004 to allow for ~12 doublings. The mixtures cultured in a shaking incubator for 24 h. The initial population and the final population were imaged using phase contrast and fluorescent microscopy. Final ratios were normalized to initial ratios where the competitive index of 1 equals no fitness change. All experiments were performed with three biological replicates.

Protein aggregation assay

In vivo protein aggregation assay was performed as described previously with slight modifications.[42] Experiments were performed as one biological replicate from each strain per experiment for three experiments. Overnights from *WT, ΔclpB, ΔpolA, and ΔclpBΔpolA* strains were back-diluted into three 50 mL PYE per strain for each timepoint (prestress, poststress, and 2h) and grown until the mid-log phase. (OD600–0.8) 40 mL from each was pelleted at 6000g for 10min at RT. Pellets were resuspended in 1 mL PYE, and poststress and 2h conditions were heat-stressed at 44°C for 15 min in a tube heater. 2h condition was reinoculated in 50 mL PYE and cultured for 2 h after stress in a shaking incubator at 30°C. All following steps were performed at 4°C and buffers used during or after cell lysis were supplemented with complete ULTRA protease inhibitor cocktail (Sigma-Aldrich). Samples

were put on ice and pelleted. (6000g, 10min) Pellets were resuspended in 1 mL of Buffer A1 (50 mM Tris/HCl pH 8.0, 150 mM NaCl, 12 U/ml Benzonase). Cells were lysed by sonication (50% amp, 10 s on/off, 6 min on time) Lysates were washed with Buffer A1 2 times after sonication to remove cell debris. (5000g, 10 min) Protein concentration was measured using Bradford assay, and 500 µL of the sample was snap-frozen in liquid nitrogen as the "total protein fraction". The remaining 500 µL was centrifuged (20000g, 20min) to pellet the insoluble protein fraction. Pellets were resuspended in 300 µL Buffer A2 (50 mM Tris/HCl pH8.0, 150 mM NaCl, %1 Triton X-100), vortexed, sonicated (high, 1 cycle, 30s), and centrifuged (20000g, 20min) for 3 times. Pellets were resuspended in 100 µL of Buffer A2, vortexed, and incubated on ice for 1 h. After a final sonication (high, 1 cycle, 30s), the samples were snap-frozen as the "insoluble protein fraction".

Ponceau and western blotting

24 µL of each protein fraction was mixed with 6 µL of 5x SDS loading dye supplemented with 5% (v/v) β-mercaptoethanol. Protein concentrations were normalized with 1x SDS loading dye relative to the sample with lowest concentration based on the Bradford assay. 10 µL of normalized samples were loaded into 12% SDS-PAGE gel after boiling for 15 min and centrifuging at max for 10–15 min. Separated proteins were transferred to nitrocellulose blotting membranes (Cytiva Amersham Protran 0.2 µm) with a semi-dry transfer unit (Hoefer). The membranes were stained by immersing in Ponceau staining solution and incubating for 20min at RT. The membranes were then washed in ultrapure water before detecting the bands with gel imager (Syngene). Destaining was done by washing the membranes with TBS-T for four times (5min). For western blotting, the membranes were blocked with 5% milk for 1h at RT, washed with TBS-T for three times, and incubated with 1:5000 anti-RecA antibody (Abcam, #ab63797) overnight at 4°C. After washing three times with TBS-T, 1:10000 IRDye 800CW goat-*anti*-rabbit IgG secondary antibody (LI-COR, #926–32211) was incubated for 1h at RT. Signals were detected by LI-COR Odyssey CLx imager after three TBS-T washes.

QUANTIFICATION AND STATISTICAL ANALYSIS

All details of the quantification and statistics used in this study are provided alongside their respective analyses in the method details section or their figure legends. All experiments were performed with at least three biological replicates unless otherwise noted. All post alignment/annotation analysis and plotting performed with R statistical software. All statistical details of the experiments are provided in their respective figure legends.

Supplementary Material

Refer to Web version on PubMed Central for supplementary material.

ACKNOWLEDGMENTS

This work was supported by National Institutes of Health grants R35GM130320 (P.C.) and R01GM135931 (P.F.). B.A was supported in part through the UMass NIH Chemistry and Biology Interface Training Program (T32GM008515). We thank the Jonas lab for sharing strains and plasmids used in this study. We also thank the Deutchbauer lab for sharing the *E. coli* strain (APA766) used in the construction of the Tn-seq library. The Chien

lab is a member of the Models to Medicine Center in the Institute for Applied Life Sciences at the University of Massachusetts Amherst.

REFERENCES

1. Shirasaki DI, Greiner ER, Al-Ramahi I, Gray M, Boontheung P, Geschwind DH, Botas J, Coppola G, Horvath S, Loo JA, and Yang XW (2012). Network Organization of the Huntingtin Proteomic Interactome in Mammalian Brain. Neuron 75, 41–57. [PubMed: 22794259]
2. Guo T, Zhang D, Zeng Y, Huang TY, Xu H, and Zhao Y. (2020). Molecular and cellular mechanisms underlying the pathogenesis of Alzheimer's disease. Mol. Neurodegener 15, 40. [PubMed: 32677986]
3. Moon HW, Han HG, and Jeon YJ (2018). Protein Quality Control in the Endoplasmic Reticulum and Cancer. Int. J. Mol. Sci 19, 3020. [PubMed: 30282948]
4. Higuchi-Sanabria R, Frankino PA, Paul JW, Tronnes SU, and Dillin A. (2018). A futile battle? Protein quality control and the stress of aging. Dev. Cell 44, 139–163. [PubMed: 29401418]
5. Nyström T, and Liu B. (2014). Protein quality control in time and space - links to cellular aging. FEMS Yeast Res. 14, 40–48. [PubMed: 24103195]
6. Reuter SH, and Shapiro L. (1987). Asymmetric segregation of heat-shock proteins upon cell division in Caulobacter crescentus. J. Mol. Biol 194, 653–662. [PubMed: 3309328]
7. Gomes SL, Juliani MH, Maia JC, and Silva AM (1986). Heat shock protein synthesis during development in Caulobacter crescentus. J. Bacteriol 168, 923–930. [PubMed: 3782032]
8. Schroeder K, and Jonas K. (2021). The Protein Quality Control Network in Caulobacter crescentus. Front. Mol. Biosci 8, 682967. [PubMed: 33996917]
9. Merdanovic M, Clausen T, Kaiser M, Huber R, and Ehrmann M. (2011). Protein Quality Control in the Bacterial Periplasm. Annu. Rev. Microbiol 65, 149–168. [PubMed: 21639788]
10. Vabulas RM, Raychaudhuri S, Hayer-Hartl M, and Hartl FU (2010). Protein Folding in the Cytoplasm and the Heat Shock Response. Cold Spring Harb. Perspect. Biol 2, a004390. [PubMed: 21123396]
11. Zeinert RD, Baniasadi H, Tu BP, and Chien P. (2020). The Lon Protease Links Nucleotide Metabolism with Proteotoxic Stress. Mol. Cell 79, 758–767.e6. [PubMed: 32755596]
12. Joshi SM, Pandey AK, Capite N, Fortune SM, Rubin EJ, and Sassetti CM (2006). Characterization of mycobacterial virulence genes through genetic interaction mapping. Proc. Natl. Acad. Sci. USA 103, 11760–11765. [PubMed: 16868085]
13. van Opijnen T, and Camilli A. (2012). A fine scale phenotype–genotype virulence map of a bacterial pathogen. Genome Res. 22, 2541–2551. [PubMed: 22826510]
14. Nolan LM, Whitchurch CB, Barquist L, Katrib M, Boinett CJ, Mayho M, Goulding D, Charles IG, Filloux A, Parkhill J, and Cain AK (2018). A global genomic approach uncovers novel components for twitching motility-mediated biofilm expansion in Pseudomonas aeruginosa. Microb. Genom 4, e000229. [PubMed: 30383525]
15. DeJesus MA, Gerrick ER, Xu W, Park SW, Long JE, Boutte CC, Rubin EJ, Schnappinger D, Ehrt S, Fortune SM, et al. (2017). Comprehensive Essentiality Analysis of the Mycobacterium tuberculosis Genome via Saturating Transposon Mutagenesis. mBio 8, e02133–16. 10.1128/mbio.02133-16. [PubMed: 28096490]
16. Poulsen BE, Yang R, Clatworthy AE, White T, Osmulski SJ, Li L, Penaranda C, Lander ES, Shoresh N, and Hung DT (2019). Defining the core essential genome of Pseudomonas aeruginosa. Proc. Natl. Acad. Sci. USA 116, 10072–10080. [PubMed: 31036669]
17. Tong AH, Evangelista M, Parsons AB, Xu H, Bader GD, Pagé N, Robinson M, Raghibizadeh S, Hogue CW, Bussey H, et al. (2001). Systematic Genetic Analysis with Ordered Arrays of Yeast Deletion Mutants. Science 294, 2364–2368. [PubMed: 11743205]
18. Giaever G, Chu AM, Ni L, Connelly C, Riles L, Véronneau S, Dow S, Lucau-Danila A, Anderson K, André B, et al. (2002). Functional profiling of the Saccharomyces cerevisiae genome. Nature 418, 387–391. [PubMed: 12140549]

19. Baba T, Ara T, Hasegawa M, Takai Y, Okumura Y, Baba M, Datsenko KA, Tomita M, Wanner BL, and Mori H. (2006). Construction of Escherichia coli K-12 in-frame, single-gene knockout mutants: the Keio collection. Mol. Syst. Biol 2, 2006.0008.
20. Sassetti CM, Boyd DH, and Rubin EJ (2001). Comprehensive identification of conditionally essential genes in mycobacteria. Proc. Natl. Acad. Sci. USA 98, 12712–12717. [PubMed: 11606763]
21. Goodman AL, McNulty NP, Zhao Y, Leip D, Mitra RD, Lozupone CA, Knight R, and Gordon JI (2009). Identifying genetic determinants needed to establish a human gut symbiont in its habitat. Cell Host Microbe 6, 279–289. [PubMed: 19748469]
22. van Opijnen T, Bodi KL, and Camilli A. (2009). Tn-seq; high-throughput parallel sequencing for fitness and genetic interaction studies in microorganisms. Nat. Methods 6, 767–772. [PubMed: 19767758]
23. Schnoes AM, Brown SD, Dodevski I, and Babbitt PC (2009). Annotation Error in Public Databases: Misannotation of Molecular Function in Enzyme Superfamilies. PLoS Comput. Biol 5, e1000605. [PubMed: 20011109]
24. Dénéréaz J, Eray E, Jana B, de Bakker V, Todor H, van Opijnen T, Liu X, and Veening JW (2024). Dual CRISPRi-Seq for genome-wide genetic interaction studies identifies key genes involved in the pneumococcal cell cycle. Cell Syst. 16, 101408.
25. Zik JJ, Price MN, Arkin AP, Deutschbauer AM, and Sham L-T (2024). Dual transposon sequencing (Dual Tn-seq) to probe genomewide genetic interactions. Preprint at bioRxiv. 10.1101/2024.09.24.614635.
26. Sanchez Y, and Lindquist SL (1990). HSP104 Required for Induced Thermotolerance. Science 248, 1112–1115. [PubMed: 2188365]
27. Squires CL, Pedersen S, Ross BM, and Squires C. (1991). ClpB is the Escherichia coli heat shock protein F84.1. J. Bacteriol 173, 4254–4262. [PubMed: 2066329]
28. Simão RCG, Susin MF, Alvarez-Martinez CE, and Gomes SL (2005). Cells lacking ClpB display a prolonged shutoff phase of the heat shock response in Caulobacter crescentus. Mol. Microbiol 57, 592–603. [PubMed: 15978087]
29. Hightower LE (1991). Heat shock, stress proteins, chaperones, and proteotoxicity. Cell 66, 191–197. [PubMed: 1855252]
30. Glover JR, and Lindquist S. (1998). Hsp104, Hsp70, and Hsp40: A Novel Chaperone System that Rescues Previously Aggregated Proteins. Cell 94, 73–82. [PubMed: 9674429]
31. Schirmer EC, Glover JR, Singer MA, and Lindquist S. (1996). HSP100/Clp proteins: a common mechanism explains diverse functions. Trends Biochem. Sci 21, 289–296. [PubMed: 8772382]
32. Ogura T, and Wilkinson AJ (2001). AAA+ superfamily ATPases: common structure–diverse function. Genes Cells 6, 575–597. [PubMed: 11473577]
33. Sarsani V, Aldikacti B, Zhao T, He S, Chien P, and Flaherty P. (2025). Discovering genetic modulators of the protein homeostasis system through multilevel analysis. PNAS Nexus 4, pgae574. [PubMed: 39807344]
34. Kantidze OL, Velichko AK, Luzhin AV, and Razin SV (2016). Heat Stress-Induced DNA Damage. Acta Naturae 8, 75–78. [PubMed: 27437141]
35. Houston BJ, Nixon B, Martin JH, De Iuliis GN, Trigg NA, Bromfield EG, McEwan KE, and Aitken RJ (2018). Heat exposure induces oxidative stress and DNA damage in the male germ line. Biol. Reprod 98, 593–606. [PubMed: 29351587]
36. de Castro Ferreira IG, Rodrigues MM, da Silva Neto JF, Mazzon RR, and do Valle Marques M. (2016). Role and regulation of ferritin-like proteins in iron homeostasis and oxidative stress survival of Caulobacter crescentus. Biometals 29, 851–862. [PubMed: 27484774]
37. Nair S, and Finkel SE (2004). Dps Protects Cells against Multiple Stresses during Stationary Phase. J. Bacteriol 186, 4192–4198. [PubMed: 15205421]
38. Silva LG, Lorenzetti APR, Ribeiro RA, Alves IR, Leaden L, Galhardo RS, Koide T, and Marques MV (2019). OxyR and the hydrogen peroxide stress response in Caulobacter crescentus. Gene 700, 70–84. [PubMed: 30880241]

39. Jensen PA, Zhu Z, and van Opijnen T. (2017). Antibiotics Disrupt Coordination between Transcriptional and Phenotypic Stress Responses in Pathogenic Bacteria. Cell Rep. 20, 1705–1716. [PubMed: 28813680]
40. Gu Z. (2022). Complex heatmap visualization. iMeta 1, e43. [PubMed: 38868715]
41. Modell JW, Kambara TK, Perchuk BS, and Laub MT (2014). A DNA Damage-Induced, SOS-Independent Checkpoint Regulates Cell Division in Caulobacter crescentus. PLoS Biol. 12, e1001977. [PubMed: 25350732]
42. Schramm FD, Heinrich K, Thüring M, Bernhardt J, and Jonas K. (2017). An essential regulatory function of the DnaK chaperone dictates the decision between proliferation and maintenance in Caulobacter crescentus. PLoS Genet. 13, e1007148. [PubMed: 29281627]
43. Da Silva ACA, Simão RCG, Susin MF, Baldini RL, Avedissian M, and Gomes SL (2003). Downregulation of the heat shock response is independent of DnaK and σ32 levels in Caulobacter crescentus. Mol. Microbiol 49, 541–553. [PubMed: 12828648]
44. Liu Y, Bauer SC, and Imlay JA (2011). The YaaA Protein of the Escherichia coli OxyR Regulon Lessens Hydrogen Peroxide Toxicity by Diminishing the Amount of Intracellular Unincorporated Iron. J. Bacteriol 193, 2186–2196. [PubMed: 21378183]
45. Tashjian TF, Zeinert RD, Eyles SJ, and Chien P. (2023). Proteomic survey of the DNA damage response in Caulobacter crescentus. J. Bacteriol 205, e0020623. [PubMed: 37730540]
46. Lehman IR, Bessman MJ, Simms ES, and Kornberg A. (1958). Enzymatic Synthesis of Deoxyribonucleic Acid: I. PREPARATION OF SUBSTRATES AND PARTIAL PURIFICATION OF AN ENZYME FROM ESCHERICHIA COLI. J. Biol. Chem 233, 163–170. [PubMed: 13563462]
47. Allen WJ, Li Y, and Waksman G. (2010). Bacterial DNA Polymerase I. In eLS (John Wiley & Sons, Ltd). 10.1002/9780470015902.a0001043.pub2.
48. Ananthaswamy HN, and Eisenstark A. (1977). Repair of hydrogen peroxide-induced single-strand breaks in Escherichia coli deoxyribonucleic acid. J. Bacteriol 130, 187–191. [PubMed: 323227]
49. Mackey BM, and Seymour DA (1987). The Effect of Catalase on Recovery of Heat-injured DNA-repair Mutants of Escherichia coli. Microbiology 133, 1601–1610.
50. Galhardo RS, Rocha RP, Marques MV, and Menck CFM (2005). An SOS-regulated operon involved in damage-inducible mutagenesis in Caulobacter crescentus. Nucleic Acids Res. 33, 2603–2614. [PubMed: 15886391]
51. Joseph AM, Daw S, Sadhir I, and Badrinarayanan A. (2021). Coordination between nucleotide excision repair and specialized polymerase DnaE2 action enables DNA damage survival in non-replicating bacteria. eLife 10, e67552. [PubMed: 33856342]
52. Reisenauer A, Mohr CD, and Shapiro L. (1996). Regulation of a heat shock sigma32 homolog in Caulobacter crescentus. J. Bacteriol 178, 1919–1927. [PubMed: 8606166]
53. Straus DB, Walter WA, and Gross CA (1987). The heat shock response of E. coli is regulated by changes in the concentration of σ32. Nature 329, 348–351. [PubMed: 3306410]
54. Wu J, and Newton A. (1996). Isolation, identification, and transcriptional specificity of the heat shock sigma factor sigma32 from Caulobacter crescentus. J. Bacteriol 178, 2094–2101. [PubMed: 8606189]
55. Schramm FD, Schroeder K, Alvelid J, Testa I, and Jonas K. (2019). Growth-driven displacement of protein aggregates along the cell length ensures partitioning to both daughter cells in Caulobacter crescentus. Mol. Microbiol 111, 1430–1448. [PubMed: 30779464]
56. Gross JD, Grunstein J, and Witkin EM (1971). Inviability of recA− derivatives of the DNA polymerase mutant of De Lucia and Cairns. J. Mol. Biol 58, 631–634. [PubMed: 4933421]
57. Monk M, and Kinross J. (1972). Conditional Lethality of recA and recB Derivatives of a Strain of Escherichia coli K-12 with a Temperature-Sensitive Deoxyribonucleic Acid Polymerase I. J. Bacteriol 109, 971–978. [PubMed: 4551758]
58. Green B, Bouchier C, Fairhead C, Craig NL, and Cormack BP (2012). Insertion site preference of Mu, Tn5, and Tn7 transposons. Mob. DNA 3, 3. [PubMed: 22313799]
59. Manna D, Porwollik S, McClelland M, Tan R, and Higgins NP (2007). Microarray analysis of Mu transposition in Salmonella enterica, serovar Typhimurium: transposon exclusion by high-density DNA binding proteins. Mol. Microbiol 66, 315–328. [PubMed: 17850262]

60. Choe D, Kim U, Hwang S, Seo SW, Kim D, Cho S, Palsson B, and Cho BK (2023). Revealing Causes for False-Positive and False-Negative Calling of Gene Essentiality in Escherichia coli Using Transposon Insertion Sequencing. mSystems 8, e0089622. [PubMed: 36507678]
61. Kimura S, Hubbard TP, Davis BM, and Waldor MK (2016). The Nucleoid Binding Protein H-NS Biases Genome-Wide Transposon Insertion Landscapes. mBio 7, e01351–16. 10.1128/mbio.01351-16. [PubMed: 27578758]
62. Mishra RC, and Grover A. (2016). ClpB/Hsp100 proteins and heat stress tolerance in plants. Crit. Rev. Biotechnol 36, 862–874. [PubMed: 26121931]
63. Meibom KL, Dubail I, Dupuis M, Barel M, Lenco J, Stulik J, Golovliov I, Sjöstedt A, and Charbit A. (2008). The heat-shock protein ClpB of Francisella tularensis is involved in stress tolerance and is required for multiplication in target organs of infected mice. Mol. Microbiol 67, 1384–1401. [PubMed: 18284578]
64. Bhat NH, Vass RH, Stoddard PR, Shin DK, and Chien P. (2013). Identification of ClpP substrates in aulobacter crescentus reveals a role for regulated proteolysis in bacterial development. Mol. Microbiol 88, 1083–1092. [PubMed: 23647068]
65. Evinger M, and Agabian N. (1977). Envelope-associated nucleoid from Caulobacter crescentus stalked and swarmer cells. J. Bacteriol 132, 294–301. [PubMed: 334726]
66. Li H, and Durbin R. (2009). Fast and accurate short read alignment with Burrows–Wheeler transform. Bioinformatics 25, 1754–1760. [PubMed: 19451168]
67. Li H, Handsaker B, Wysoker A, Fennell T, Ruan J, Homer N, Marth G, Abecasis G, and Durbin R. (2009). The Sequence Alignment/Map Format and SAMtools. Bioinformatics 25, 2078–2079. [PubMed: 19505943]
68. Quinlan AR, and Hall IM (2010). BEDTools: a flexible suite of utilities for comparing genomic features. Bioinformatics 26, 841–842. [PubMed: 20110278]
69. Girardot C, Scholtalbers J, Sauer S, Su S-Y, and Furlong EEM (2016). Je, a versatile suite to handle multiplexed NGS libraries with unique molecular identifiers. BMC Bioinf. 17, 419.
70. Shen W, Sipos B, and Zhao L. (2024). SeqKit2: A Swiss army knife for sequence and alignment processing. iMeta 3, e191. [PubMed: 38898985]
71. Ramírez F, Dündar F, Diehl S, Grüning BA, and Manke T. (2014). deepTools: a flexible platform for exploring deep-sequencing data. Nucleic Acids Res. 42, W187–W191. [PubMed: 24799436]
72. Chen S. (2023). Ultrafast one-pass FASTQ data preprocessing, quality control, and deduplication using fastp. iMeta 2, e107. [PubMed: 38868435]
73. Liao Y, Smyth GK, and Shi W. (2019). The R package Rsubread is easier, faster, cheaper and better for alignment and quantification of RNA sequencing reads. Nucleic Acids Res. 47, e47. [PubMed: 30783653]
74. Molder F, Jablonski KP, Letcher B, Hall MB, van Dyken PC, Tomkins-Tinch CH, Sochat V, Forster J, Vieira FG, Meesters C, et al. (2021). Sustainable Data Analysis with Snakemake. F1000Research 10, 33. [PubMed: 34035898]
75. Di Tommaso P, Chatzou M, Floden EW, Barja PP, Palumbo E, and Notredame C. (2017). Nextflow enables reproducible computational workflows. Nat. Biotechnol 35, 316–319. [PubMed: 28398311]
76. Anders S, and Huber W. (2010). Differential expression analysis for sequence count data. Genome Biol. 11, R106. [PubMed: 20979621]
77. Zhang Y, Parmigiani G, and Johnson WE (2020). ComBat-seq: batch effect adjustment for RNA-seq count data. NAR Genom. Bioinform 2, lqaa078. [PubMed: 33015620]
78. Skerker JM, Prasol MS, Perchuk BS, Biondi EG, and Laub MT (2005). Two-Component Signal Transduction Pathways Regulating Growth and Cell Cycle Progression in a Bacterium: A System-Level Analysis. PLoS Biol. 3, e334. [PubMed: 16176121]
79. Ely B, and Johnson RC (1977). Generalized Transduction in CAULOBACTER CRESCENTUS. Genetics 87, 391–399. [PubMed: 17248770]
80. Hentchel KL, Reyes Ruiz LM, Curtis PD, Fiebig A, Coleman ML, and Crosson S. (2019). Genome-scale fitness profile of Caulobacter crescentus grown in natural freshwater. ISME J. 13, 523–536. [PubMed: 30297849]

81. Love MI, Huber W, and Anders S. (2014). Moderated estimation of fold change and dispersion for RNA-seq data with DESeq2. Genome Biol. 15, 550. [PubMed: 25516281]

Highlights

- Tn-seq in PQC-deficient cells exposes hidden genes needed for proteotoxic stress tolerances
- DNA repair is particularly important for oxidative stress tolerance in the absence of Lon
- Synthetic lethality links ClpB and PolA to RecA aggregation during strong heat shock
- Protein aggregation lethality is specific to individual genetic or environmental backgrounds

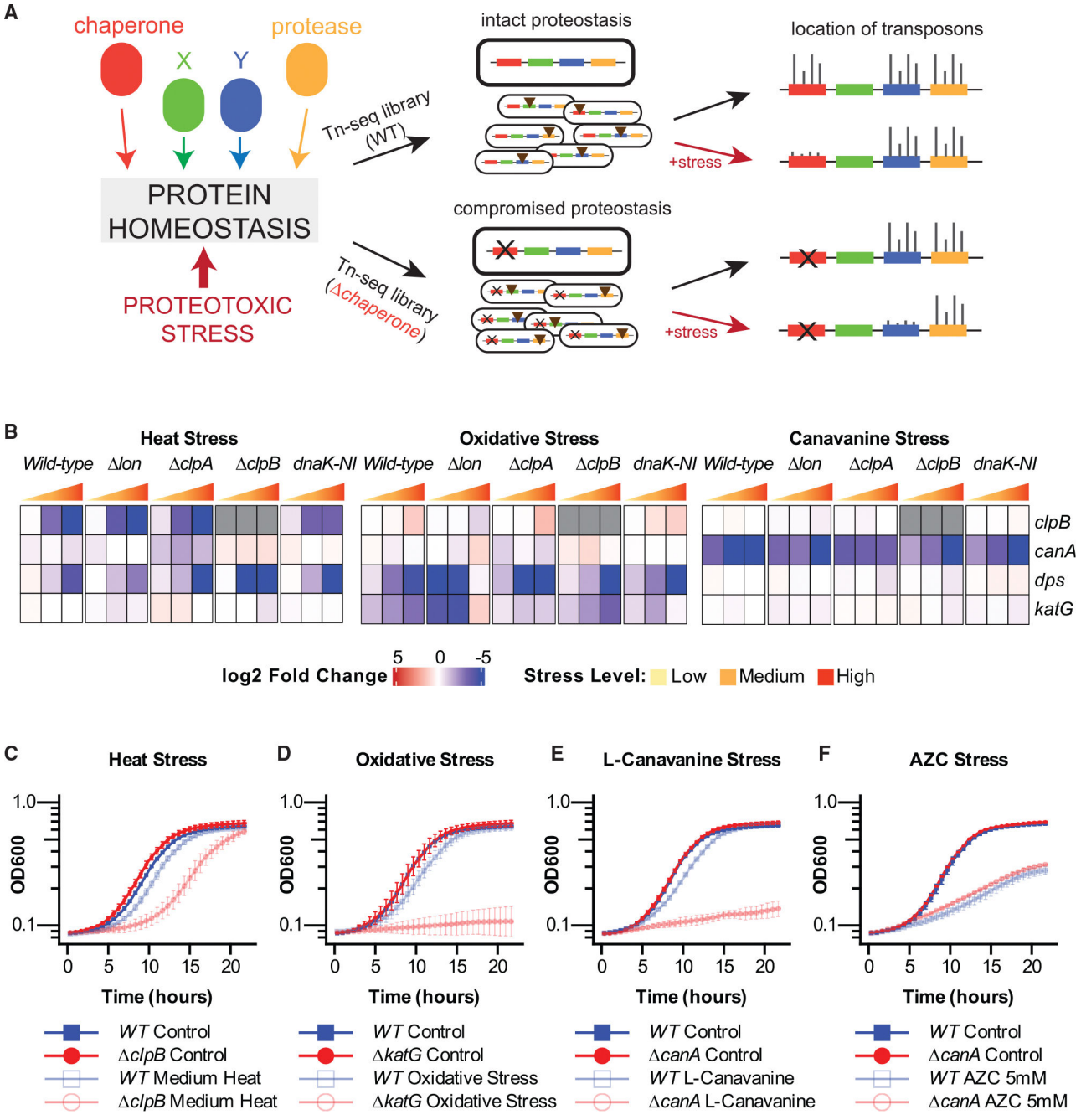

Figure 1. Global proteotoxic stress fitness determinants in *Caulobacter crescentus*

(A) Maintaining cellular proteostasis requires the contribution of chaperones, proteases, and other proteins. Transposon insertion libraries result in single disruptions in every cell (middle), the position of which can be deconvoluted through sequencing and the number of insertions quantified (right). In wild-type cells, the importance of major genes during specific proteotoxic stress responses is revealed (top shows that the red chaperone gene is important for stress tolerance, while blue protein Y is not). Generating these libraries in cells compromised in proteostasis due to loss of a factor (red chaperone in this case) and

subjected to the same proteotoxic stress unmasks the hidden players in the response (blue protein Y is important in the absence of the red chaperone protein in this illustration).
(B) Heatmaps showing fitness scores (log2 fold change) of genes from −5 (blue) to +5 (red) range for the mutant library independent stress determinants. Fold changes are calculated by subtracting the log2 median batch-corrected transposon insertion count of the stress condition from that of the mutant library control condition. ClpB insertions under the Δ*clpB* strain are greyed out to indicate that there are no insertions in the *clpB* gene in that strain. The yellow, orange, and red triangles on the heatmaps show the stress level for each condition. In the order of low-medium-high, the stress levels are as follows: heat stress (37°C, 42°C, and 43.8°C), oxidative stress (0.025, 0.05, and 0.1 mM), and l-canavanine stress (25, 50, and 100 μg/ml).
(C–F) Bacterial growth curves (OD600) showing mean ± standard deviation from three biological replicates of (C) *WT* and *ΔclpB* strains under medium heat stress (42°C 45 min), (D) *WT* and Δ*katG* strains under medium oxidative stress (0.05 mM H_2O_2, chronic), (E) *WT* and Δ*canA* strains under medium l-canavanine stress (50 μg/mL, chronic), and (F) *WT* and Δ*canA* under azetidine-2-carboxylic acid (AZC) stress (5 mM, chronic).
See also Figures S1–S3.

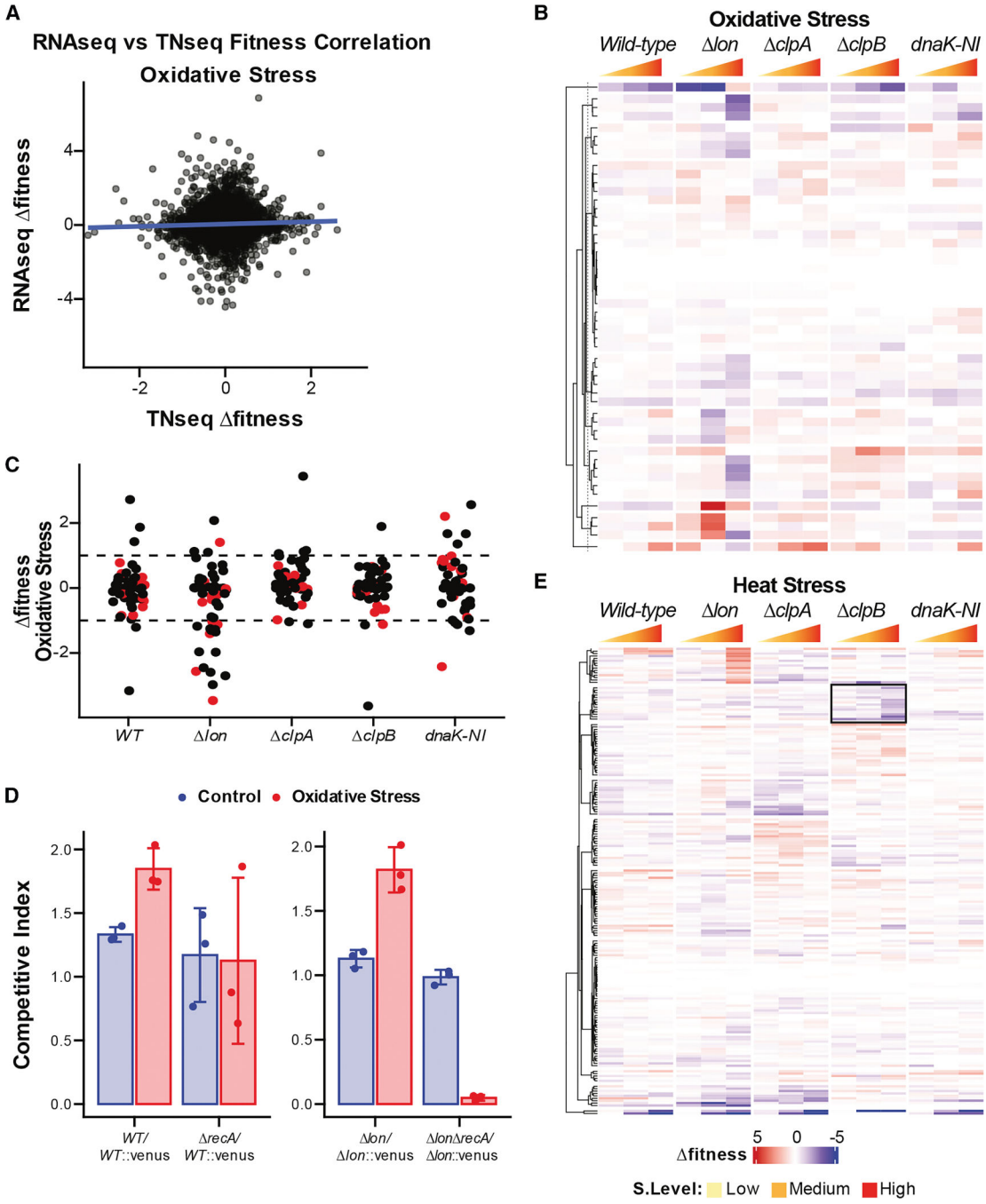

Figure 2. Loss of Lon protease uncovers synergism between oxidative stress and DNA damage

(A) Scatterplot compares the log2 fold change from *WT* oxidative stress transcriptomic data and *WT* oxidative stress Tnseq data. The blue line indicates the linear fitted line to all of the data. Transcriptomic data were obtained from Silva et al.,[38] in which the *WT* 15-min H_2O_2 condition was compared to the *WT* control.

(B and C) The oxidative stress regulon obtained from Silva et al.[38] is used to compare transcriptomic changes with fitness. The differentially expressed genes were obtained by comparing the *WT* 15-min H_2O_2 condition to the *WT* control. (B) Heatmap shows the

log2 fold changes of batch-corrected transposon insertion counts (Δfitness) for low, medium, and high oxidative stress conditions for *WT, Δlon, ΔclpA, ΔclpB*, and *dnaK-NI* transposon libraries. The heatmap was generated using the ComplexHeatmap[40] R package. Rows were hierarchically clustered using Euclidean distance and complete linkage. (C) Fitness values from high oxidative stress are plotted as dots to highlight the distribution between strains. Dashed lines indicate fitness at −1 and +1. Red dots highlight the DNA damage response genes identified by Modell et al.[41]

(D) *In vivo* competition experiments for *WT*, *ΔrecA*, *Δlon*, and *ΔlonΔrecA* strains under 0.025 mM H_2O_2 stress were conducted, with the competitive index as the output parameter. The experiment involved mixing the strains *WT-WT::venus*, *ΔrecA-WT::venus*, *Δlon-Δlon::venus*, and *ΔlonΔrecA-Δlon::venus* in a 1:1 ratio and growing them for 24 h. Image quantification of the ratio of fluorescent to non-fluorescent cells was performed at the time of mixing and after 24 h of growth to calculate the competitive index. Each dot represents a biological replicate, bars show the mean, and the error bars indicate standard deviation.

(E) RpoH regulon obtained from Schramm et al.[42] and used to compare transcriptomic changes with fitness. Heatmap shows the log2 fold changes of batch-corrected transposon insertion counts for low, medium, and high oxidative stress conditions for *WT*, *Δlon*, *ΔclpA*, *ΔclpB*, and *dnaK-NI* transposon libraries. The black box highlights the cluster of genes that cause a negative fitness change in the *ΔclpB* background. This cluster includes the genes *yaaA* and *oxyR*. The heatmap was generated using the ComplexHeatmap[40] R package. Rows were hierarchically clustered using Euclidean distance and complete linkage.

See also Figures S4–S6.

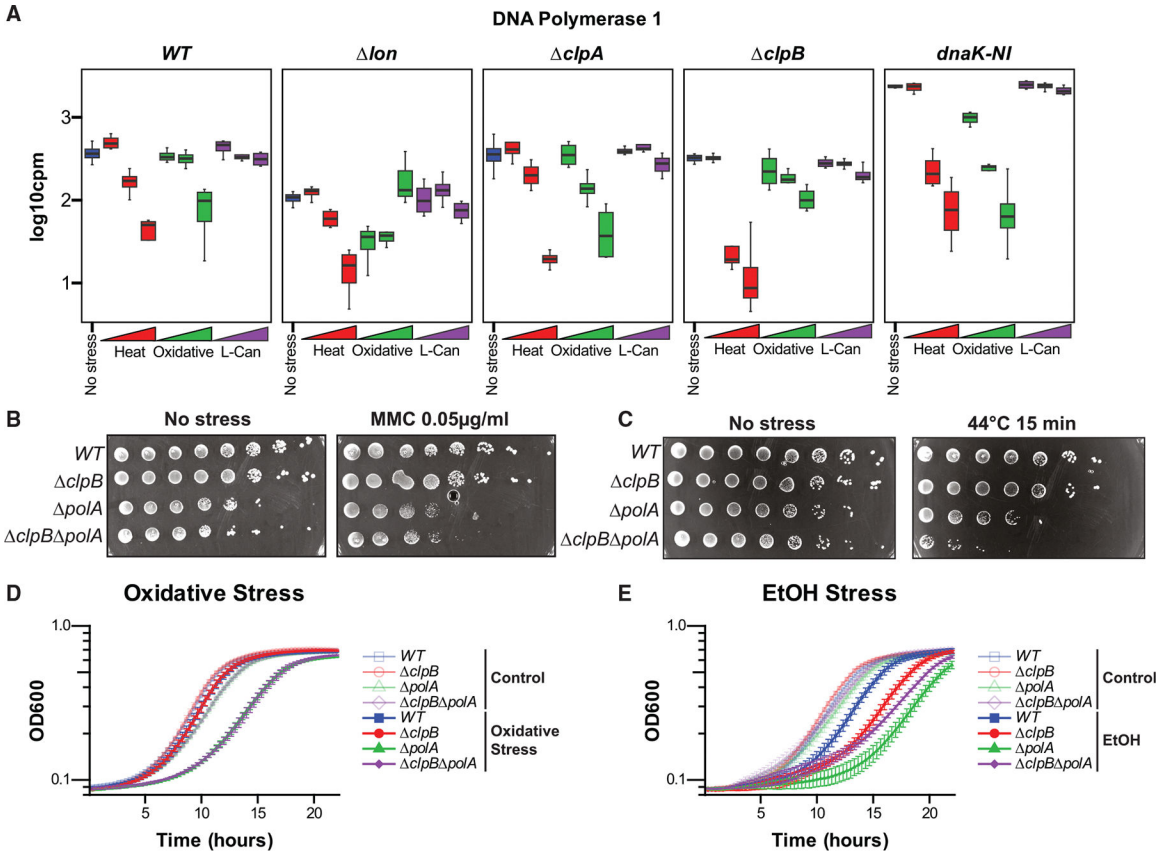

Figure 3. DNA polymerase 1 is sensitive to heat and oxidative stresses and shows a synergistic fitness defect with ClpB under heat stress

(A) DNA polymerase 1 (PolA) transposon insertion profile across all tested transposon mutagenesis libraries and stresses. Insertion counts are presented as log10 counts per million after batch correction. Stress conditions are color-coded, depicting low-, medium-, and high stress levels through the triangle. Boxplots show the median and interquartile range, and whiskers extend to all data points not considered outliers.

(B) Spot titration (10-fold dilution series) of *WT*, *ΔclpB*, *ΔpolA*, and *ΔclpBΔpolA* strains under 0.05 μg/mL chronic mitomycin C (MMC) stress.

(C) Spot titration (10-fold dilution series) of *WT*, *ΔclpB*, *ΔpolA*, and *ΔclpBΔpolA* strains under 44°C heat stress for 15 min.

(D) Growth curves (OD600) *of WT*, *ΔclpB*, *ΔpolA*, and *ΔclpBΔpolA* strains under chronic 0.05 mM H_2O_2 stress. Results are shown as mean ± standard deviation.

(E) Growth curves (OD600) of *WT*, *ΔclpB*, *ΔpolA*, and *ΔclpBΔpolA* strains under 20% EtOH stress for 15 min. Results are shown as mean ± standard deviation.

See also Figure S7.

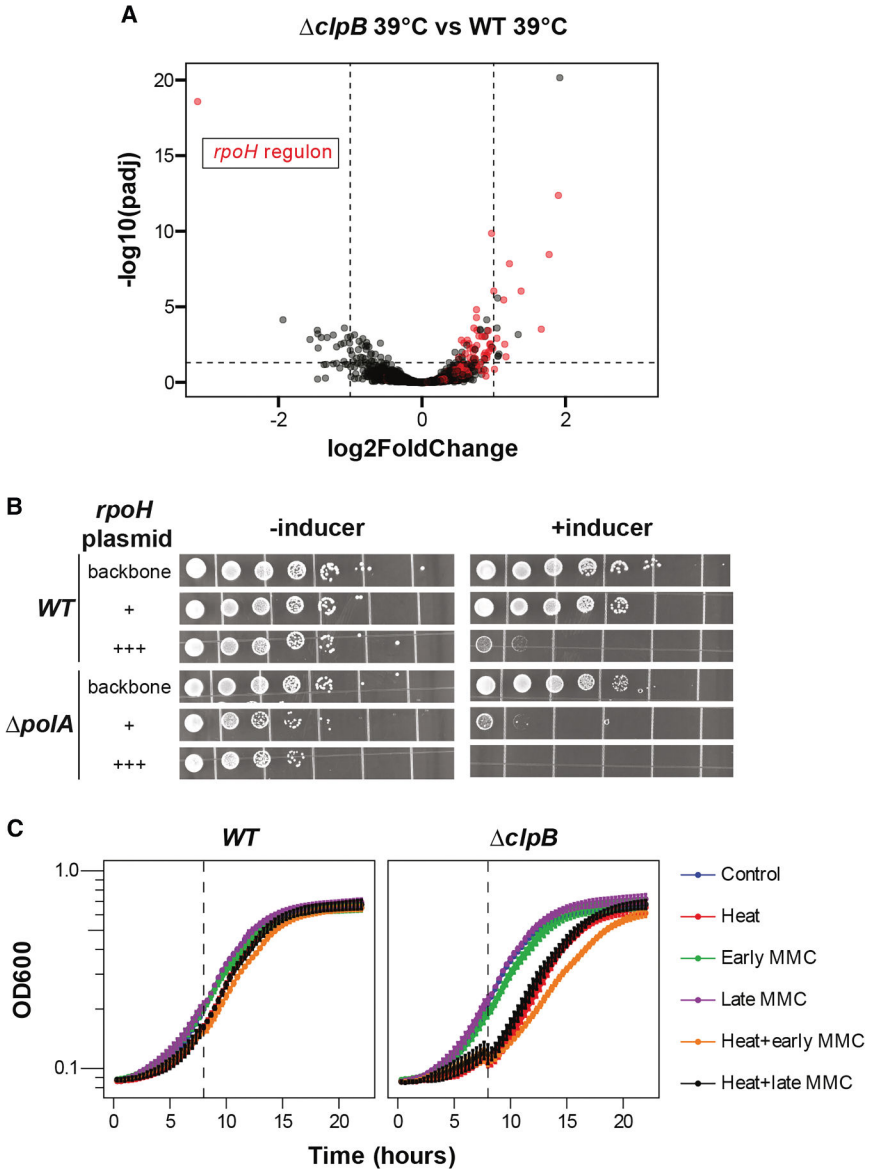

Figure 4. Consistent *rpoH* expression contributes to the synergistic PolA ClpB heat stress phenotype

(A) Total RNA sequencing was performed to identify transcriptomic differences between Δ*clpB* and *WT* strains under heat stress (39°C, chronic). The *rpoH* regulon obtained from Schramm et al.[42] is highlighted on the volcano plot in red. The *x* axis shows the log2 fold change, and the *y* axis shows the −log10 adjusted *p* value. Vertical black dashed lines drawn at ±1 log2 fold change, and horizontal lines are drawn at a value corresponding to a 0.05 adjusted *p* value.

(B) Spot titration (10-fold serial dilutions) with *WT* and Δ*polA* strains carrying *rpoH* overexpression plasmids. Vanillate (0.5 mM) was used as the inducer, and chloramphenicol (1 μg/ml) was used as the selection. Strains contain plasmids for vanillate-inducible *rpoH* (+), non-degradable *rpoH* (*rpoHV56A; +++*), or the backbone plasmid as control. A representative image from one of the three biological replicates is shown for each condition.

(C) Growth curves (OD600) of *WT* and Δ*clpB* strains under heat (44°C, 15 min), early MMC (added at 0 h, 0.05 μg/ml, chronic), late MMC (added at 8 h, 0.05 μg/ml, chronic), and combinations of heat and early or late MMC conditions. The dashed line indicates the late MMC addition at 8 h. Results are shown as mean ± standard deviation.
See also Figures S8–S11, and Table S3.

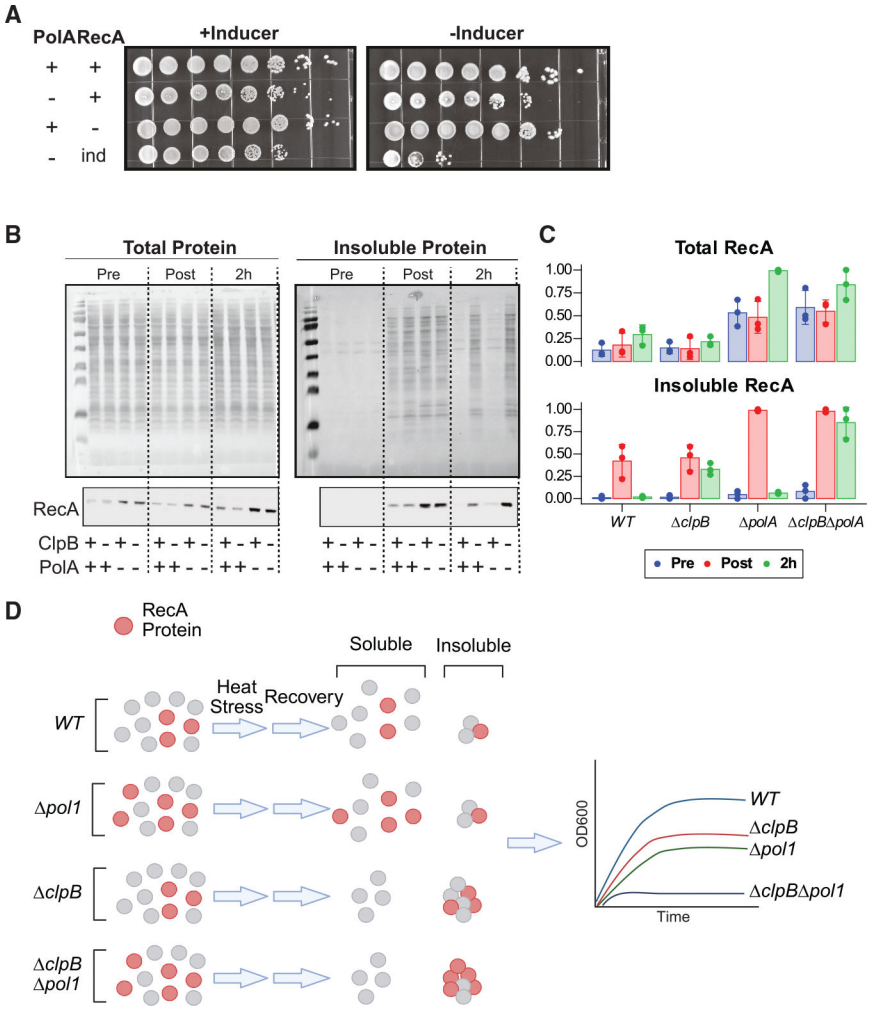

Figure 5. Heat-induced aggregation of RecA in Δ*clpB* causes increased sensitivity to heat stress in the absence of PolA

(A) Spot titrations (10-fold serial dilutions) with *WT* or cells lacking RecA or PolA or both in an inducible RecA background. "+/−" indicates the presence or absence of PolA or RecA, and "++" indicates *WT* strains. 0.2% Xylose was used as the inducer, and 0.2% glucose was used to suppress the leaky expression of the xylose promoter in the "-Inducer" condition. "ind" in the legend indicates inducible RecA.

(B) Total and insoluble protein fractions collected from *WT*, *ΔclpB*, *ΔpolA*, and *ΔclpBΔpolA* strains before heat stress (44°C, 15 min) (**pre**), immediately after heat stress (**post**), and 2 h (**2h**) after heat stress. Ponceau stain was used to identify total protein (upper panel), and western blots were used for RecA proteins. (Lower panel) Quantifications were performed by normalizing RecA levels to the total protein and are shown in the right panel as bar plots. A representative blot from one of the three biological replicates is shown for each condition.

(C) RecA western blot quantifications are shown from Figure 5A (lower panel). Dots represent individual biological replicates, and error bars represent standard deviation.

(D) Cartoon schematic of how RecA aggregation in ΔclpB strains leads to depletion of RecA from the soluble pool.

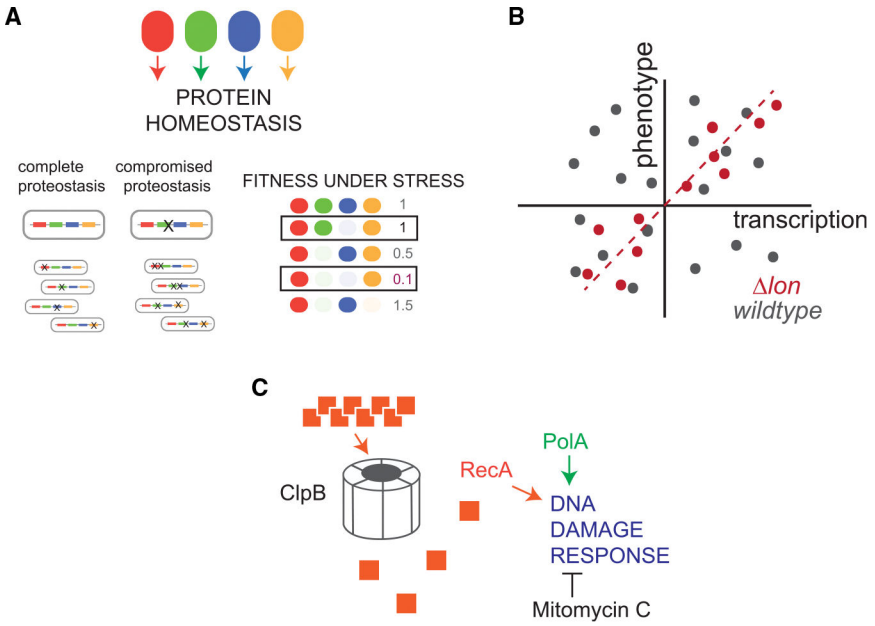

Figure 6. Systematic fitness profiling across protein quality control mutants uncovers masked genetic dependencies linking heat stress tolerance and genome stability

(A) Unmasking vulnerable genes arise from the use of strains deficient in PQC components under environmental conditions that specifically stress protein homeostasis. This approach uncovers new genes that affect stress responses, correlations in phenotypes, and transcription under vulnerable conditions (B) and deepens the understanding of intersections between heat-stress tolerance and DNA damage responses (C).

KEY RESOURCES TABLE

REAGENT or RESOURCE	SOURCE	IDENTIFIER
Antibodies		
Rabbit polyclonal anti-RecA primary antibody	Abcam	Cat# ab63797; RRID: AB_1142554
Rabbit polyclonal anti-ClpP primary antibody	Bhat et al.[64]	N/A
Goat polyclonal anti-rabbit secondary antibody	LI-COR	Cat# 926-32211; RRID: AB_621843
Bacterial and virus strains		
Caulobacter crescentus CB15N/NA1000 (WT)	Evinger and Agabian[65]	CPC176
NA1000 Δlon	Lab collection	CPC667
NA1000 ΔclpA (SpecR)	Lab collection	CPC389
NA1000 ΔclpB, dnaK::dnaK-GSG-mVenus (tetR)	Schramm et al.[55]	CPC1008
NA1000 ΔclpB (tetR)	This study	CPC1019
NA1000 ΔdnaK, pXyl::dnaK (dnaK-NI) (specR)	Da Silva et al.[43]	CPC237
NA1000 ΔkatG (gentR)	This study	CPC1020
NA1000 ΔlonΔclpB	This study	CPC1301
NA1000 ΔclpAΔclpB	This study	CPC1306
NA1000 ΔclpBΔdnaK, pXyl::dnaK	This study	CPC1307
NA1000 ΔlonΔkatG (gentR)	Lab collection	CPC1227
NA1000 ΔclpAΔkatG (specR, gentR)	This study	CPC1294
NA1000 ΔclpBΔkatG (tetR, gentR)	This study	CPC1295
NA1000 dnaKNIΔkatG (specR, gentR)	This study	CPC1292
NA1000 ΔpolA (gentR)	This study	CPC1190
NA1000 ΔclpBΔpolA (tetR, gentR)	This study	CPC1193
NA1000 Δdps (gentR)	This study	CPC1277
NA1000 ΔlonΔdps (gentR)	This study	CPC1297
NA1000 ΔclpAΔdps (specR, gentR)	This study	CPC1302
NA1000 ΔclpBΔdps (tetR, gentR)	This study	CPC1298
NA1000 dnakNIΔdps (specR, gentR)	This study	CPC1303
NA1000 ΔcanA (gentR)	This study	CPC1276
NA1000 ΔlonΔcanA (gentR)	This study	CPC1299
NA1000 ΔclpAΔcanA (specR, gentR)	This study	CPC1304
NA1000 ΔclpBΔcanA (tetR, gentR)	This study	CPC1300
NA1000 dnakNIΔcanA (specR, gentR)	This study	CPC1305
NA1000 ΔrecA (gentR)	Lab collection	CPC556
NA1000 ΔlonΔrecA (gentR)	Lab collection	CPC562
NA1000 ΔrecA, pXyl::recA (chlorR, kanR)	This study	CPC1265
NA1000 ΔpolAΔrecA, pXyl::recA (gentR, chlorR, kanR)	This study	CPC1311
NA1000 plac::venus (kanR)	Lab collection	CPC798
NA1000 Δlon, plac::venus (kanR)	Lab collection	CPC807
NA1000 pJS14 (chlorR)	This study	CPC1249

REAGENT or RESOURCE	SOURCE	IDENTIFIER
NA1000 pJS14-pVan-rpoH (chlorR)	This study	CPC1247
NA1000 pJS14-pVan-rpoHB56A (chlorR)	This study	CPC1248
NA1000 ΔpolA, pJS14 (chlorR)	This study	CPC1252
NA1000 ΔpolA, pJS14-pVan-rpoH (chlorR)	This study	CPC1250
NA1000 ΔpolA, pJS14-pVan-rpoHB56A (chlorR)	This study	CPC1251
NA1000 ΔdnaE2	This study	CPC1176
NA1000 ΔclpBΔdnaE2 (tetR)	This study	CPC1312
NA1000 ΔpolAΔdnaE2 (gentR)	This study	CPC1313
NA1000 ΔclpBΔpolAΔdnaE2 (tetR, gentR)	This study	CPC1314
TOP10 pJS14 high copy plasmid (chlorR)	Schramm et al.[42]	EPC1774
TOP10 pJS14-rrnB1B2-PvanR-VanR-PvanA-rpoH-T500, vector for vanillate-dependent overexpression of rpoH (chlorR)	Schramm et al.[42]	EPC1770
TOP10 pJS14-rrnB1B2-PvanR-VanR-PvanA-rpoHV56A-T500, vector for vanillate-dependent overexpression of rpoHV56A (chlorR)	Schramm et al.[42]	EPC1771
Chemicals, peptides, and recombinant proteins		
Mitomycin C	Sigma	Cat #M0503
Hydrogen peroxide	Fisher Scientific	Cat #BP2633500
complete ULTRA protease inhibitor cocktail	Sigma	Cat #5892970001
Benzonase	Merck Millipore	Cat #70746
2,6-Diaminopimelic acid (DAP)	Sigma	Cat #D1377-5G
Critical commercial assays		
Monarch Genomic DNA isolation kit	NEB	Cat #T3010L
NEBuilder HiFi Gibson Assembly mix	NEB	Cat #2621L
Aline PCRClean DX magnetic beads	Aline Biosciences	Cat #C-1003-50
Coomassie Plus (Bradford) Protein Assay	ThermoFisher Scientific	Cat #23236
NextSeq 500/550 High Output Kit v2.5 (75 Cycles)	Illumina	Cat #20024906
Illumina Stranded Total RNA Prep with Ribo-Zero Plus	Illumina	Cat #20040529
Deposited data		
Transposon sequencing data	Sarsani et al.[33]	GSE244581
RNA sequencing data	This study	GSE312471
Oligonucleotides		
See Table S2 for primers used in the transposon mutagenesis sequencing	This study	N/A
See Table S2 for primers for preparing knock-out strains	This study	N/A
Recombinant DNA		
pNTPS138_ΔpolA_gentR	This study	N/A
pNTPS138_ΔkatG_gentR	This study	N/A
pJS14 high copy plasmid (chlorR)	Schramm et al.[55]	N/A

REAGENT or RESOURCE	SOURCE	IDENTIFIER
pJS14-rrnB1B2-PvanR-VanR-PvanA-rpoH-T500, vector for vanillate-dependent overexpression of rpoH (chlorR)	Schramm et al.[55]	N/A
pJS14-rrnB1B2-PvanR-VanR-PvanA-rpoHV56A-T500, vector for vanillate-dependent overexpression of rpoHV56A (chlorR)	Schramm et al.[55]	N/A
Software and algorithms		
GraphPad Prism	Dotmatics	https://www.graphpad.com/features
Gen6 Software	Agilent	N/A
R	The R Foundation	https://www.r-project.org/
BWA	Li and Durbin[66]	https://bio-bwa.sourceforge.net/
Samtools	Li et al., 2009[67]	http://www.htslib.org/
BEDTools	Quinlan and Hall[68]	https://bedtools.readthedocs.io/en/latest/
JE	Girardot et al.[69]	https://github.com/gbcs-embl/Je
Seqkit	Shen et al.[70]	https://bioinf.shenwei.me/seqkit/
Deeptools	Ramirez et al.[71]	https://deeptools.readthedocs.io/en/latest/
Fastp	Chen et al.[72]	https://github.com/OpenGene/fastp
R package (Rsubread)	Liao et al.[73]	https://doi.org/10.18129/B9.bioc.Rsubread
Snakemake	Molder et al.[74]	https://snakemake.readthedocs.io/en/stable/
Nextflow	Di Tammaso et al.[75]	https://www.nextflow.io/
chienlab-rnaseq	This study	https://doi.org/10.5281/zenodo.17809427
chienlab-tnseq	Sarsani et al.[33]	https://doi.org/10.5281/zenodo.17852222
R package (DESeq2)	Anders and Huber[76]	https://doi.org/10.18129/B9.bioc.DESeq2
R package (ComBat-seq, sva)	Zhang et al.[77]	https://doi.org/10.18129/B9.bioc.sva
R package (ComplexHeatmap)	Gu[40]	https://doi.org/10.18129/B9.bioc.ComplexHeatmap
Adobe Illustrator	Adobe	RRID:SCR_010279